

Article

Valorization of (Bio)Ethanol over $\text{MoO}_3/(\text{WO}_3\text{-ZrO}_2)$ Sol-Gel-like Catalysts

Ana Paula Soares Dias ^{1,2,*} , Bruna Rijo ² , Manuel Francisco Costa Pereira ¹, Rodica Zăvoianu ³ 
and Octavian Dumitru Pavel ³ 

¹ Centro de Recursos Naturais e Ambiente (CERENA), Instituto Superior Técnico, University of Lisbon, Av. Rovisco Pais, 1, 1049-001 Lisboa, Portugal; mfcpc@tecnico.ulisboa.pt

² Centro de Investigação para a Valorização de Recursos Endógenos (VALORIZA), Polytechnic Institute of Portalegre, Campus Politécnico, 10, 7300-555 Portalegre, Portugal; bruna.rijo@ippportalegre.pt

³ Department of Inorganic Chemistry, Organic Chemistry, Biochemistry and Catalysis, Faculty of Chemistry, University of Bucharest, 4-12 Regina Elisabeta Bd., 030018 Bucharest, Romania; rodica.zavoianu@chimie.unibuc.ro (R.Z.); octavian.pavel@chimie.unibuc.ro (O.D.P.)

* Correspondence: apsoares@tecnico.ulisboa.pt

Abstract: Bioethanol, which is currently produced commercially from a growing variety of renewable biomass and waste sources, is an appealing feedstock for the production of fuels and chemicals. The literature clearly shows that bioethanol is a versatile building block to be used in biorefineries. The ethanol conversion using several catalysts with acidic, basic, and redox characteristics results in a diverse assortment of high-value bioproducts. High-acidity tungsten zirconia-based catalysts are stated to compete with traditional zeolitic catalysts and can be employed in the dehydration of ethanol to ethylene, but for a low reaction temperature acetic acid is formed, which causes corrosion issues. $\text{WO}_3\text{-ZrO}_2$ ($W/Zr = 1$, atomic) catalysts modified with MoO_3 were prepared by a sol-gel-like procedure and tested in a gas phase ethanol conversion in the presence of air. The citrate derived xerogels were annealed at 853 K for 12 h, allowing low surface area ($<10 \text{ m}^2/\text{g}$) materials with a Mo-W mixed-oxide-rich surface over tetragonal nanostructured zirconia. Catalysts with MoO_3 -loading produced mainly acetaldehyde, instead of ethylene, as a result of the high reducibility of Mo^{6+} when compared to W^{6+} . During the reaction, the Mo^{6+} becomes partially reduced, but $\text{Mo}^{6+}/\text{Mo}^{5+}$ species are still active for methanol conversion with increased ethylene selectivity due to the high acidity of tetrahedral MO_X species formed during the reaction. Adding water to ethanol, to simulate bioethanol, only leads to a slight inhibition in ethanol conversion over the $\text{MoO}_3/(\text{WO}_3\text{-ZrO}_2)$ catalysts. The results show that molybdenum oxide deposited on tungstated zirconia catalyst is active, with low sensitivity to water, for the valorization of bioethanol into high-value chemicals, such as ethylene and acetaldehyde, and whose selectivity can be tuned by changing the amount of MoO_3 that is loaded. The $\text{MoO}_3/(\text{WO}_3\text{-ZrO}_2)$ catalysts prepared show catalytic behavior similar to that of noble metal-based catalysts reported in the literature for the dehydrogenation of bioethanol in high-value chemicals.

Keywords: bioethanol valorization; ethylene; acetaldehyde; sol-gel catalysts; $\text{WO}_3\text{-ZrO}_2$; dehydrogenation; dehydration



Citation: Soares Dias, A.P.; Rijo, B.; Costa Pereira, M.F.; Zăvoianu, R.; Pavel, O.D. Valorization of (Bio)Ethanol over $\text{MoO}_3/(\text{WO}_3\text{-ZrO}_2)$ Sol-Gel-like Catalysts. *Reactions* **2024**, *5*, 260–273. <https://doi.org/10.3390/reactions5010012>

Academic Editors: Ioannis V. Yentekakis and Dmitry Yu. Murzin

Received: 15 January 2024

Revised: 8 February 2024

Accepted: 11 March 2024

Published: 20 March 2024



Copyright: © 2024 by the authors. Licensee MDPI, Basel, Switzerland. This article is an open access article distributed under the terms and conditions of the Creative Commons Attribution (CC BY) license (<https://creativecommons.org/licenses/by/4.0/>).

1. Introduction

Given that oil and its derivatives are responsible for global warming and adverse climate change, today's civilization faces significant hurdles in terms of the energy and chemical sources that are critical to sustaining a high socioeconomic level. Ethanol, bio, currently produced commercially from a growing variety of renewable biomass and waste sources, is an appealing feedstock for the production of fuels and chemicals [1]. The data reported in the literature clearly show that bioethanol is a versatile building block to be used in biorefineries [2] (Figure 1). According to Posada et al. [2], the 1,3 butadiene and diethyl ether are the most promising ethanol derivatives followed by ethylene, propylene,

acetaldehyde, ethylene oxide, and ethyl acetate. A more recent evaluation of the potential profitability of ethanol-derived chemicals indicates a different point of view where ethylene is a non-profitable ethanol-derived product [3]. Many factors influence the economic feasibility of each of the conceivable ethanol-derived products, such that Frosi et al. [4] identified ethanol diluted in water as the most cost-effective approach for the viability of ethylene synthesis.

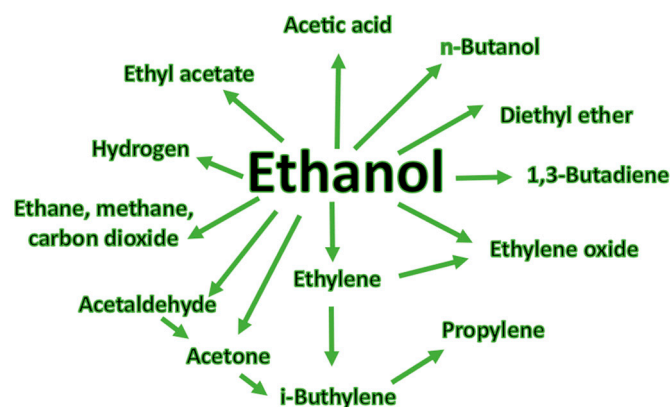


Figure 1. Ethanol as a building block in a biorefinery concept (adapted from [2]).

Ethanol can be converted in different catalyzed processes including dehydrogenation, C–C bond coupling, aromatization, hydrogen transfer, and dehydration [5]. The ethanol dehydrogenation and dehydration reactions are widely used as model reactions to characterize acidic and basic catalysts [6]. Acid catalysts promote ethanol dehydration to ethylene and, at low temperatures, produce diethyl ether. Basic catalysts promote ethanol dehydrogenation to form acetaldehyde. For metal oxide catalysts, the ethanol dehydration and dehydrogenation mechanisms are schematized in Figure 2.

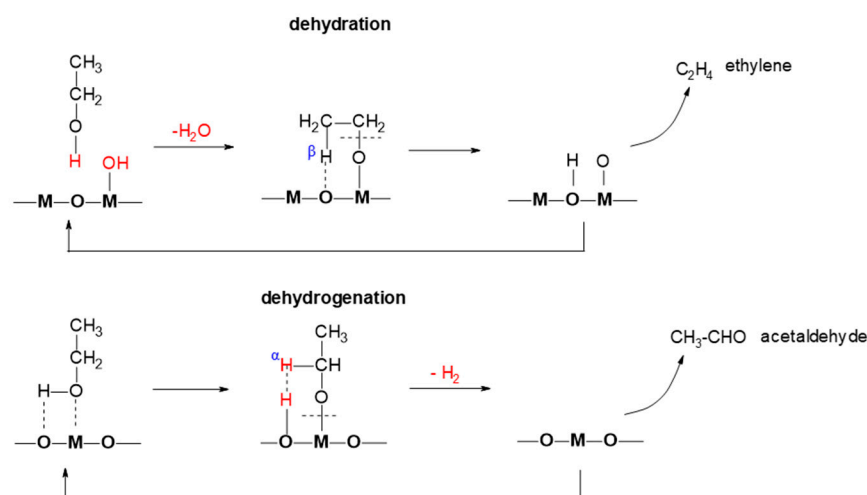


Figure 2. Ethanol dehydration and dehydrogenation reaction mechanisms over methanol oxide catalysts (adapted from [6]).

Different metal oxides present different catalytic activities for both reactions (Table 1). By combining different metal oxides, it is possible to obtain catalysts with morphologies and solid-state properties that give them catalytic performance, such as activity, selectivity, and stability, for a given reaction [7].

Table 1. Dehydration and dehydrogenation abilities of different metal oxide catalysts (adapted from [6]).

Metal Oxide	Dehydration (%)	Dehydrogenation (%)
ThO ₂	100	trace
Al ₂ O ₃	98.5	1.5
W ₂ O ₄	98.5	1.5
Cr ₂ O ₃	91	9
SiO ₂	84	16
TiO ₂	63	37
BeO	45	55
ZrO ₂	45	55
UO ₂	24	76
Mo ₂ O ₅	23	77
Fe ₂ O ₃	14	86
V ₂ O ₅	9	91
ZnO	5	95
MnO	0	100
SnO	0	100
CdO	0	100
Mn ₃ O ₅	0	100
MgO	0	100

Phung et al. [8] investigated ethanol dehydrogenation over WO₃/ZrO₂ and WO₃/TiO₂ catalysts. The authors reported the formation of strong Brønsted acid sites when both zirconia and titania were modified with WO₃. Such strong acidity prevents the formation of byproducts, making these catalysts serious competitors to conventional zeolitic acid catalysts. Combining theoretical computations with experimental nanoscopic characterization techniques, Zhou et al. [9] describe the active sites of a WO₃/ZrO₂ catalyst as Zr-WO_x agglomerates of around 1 nm; thus, the catalytic activity is being strongly influenced by the W species surface density and by the preparation methodology. Rousseau et al. [10] compared the catalytic behavior of W⁶⁺ and Mo⁶⁺ clusters in the dehydrogenation and dehydration of alcohols such as ethanol. The authors concluded that the strong Lewis acidity of W⁶⁺ relative to Mo⁶⁺ makes tungsten clusters more active than molybdenum analogs, but the higher reducibility of Mo⁶⁺ increases the selectivity of molybdenum clusters towards oxidation reactions, such as ethanol to acetaldehyde, which is a valuable chemical.

Chuklina et al. [11] used (Zr+Ce)/Al₂O₃ mixed-oxide catalysts, prepared by the sol-gel method, to convert ethanol into ethylene, acetaldehyde, and diethyl ether. For low temperatures, the researchers reported a competition between dehydration and dehydrogenation reaction paths because ethylene and acetaldehyde have the same reaction intermediate. Catalysts with low ZrO₂ content promoted the selectivity towards diethyl ether, which was produced over Al³⁺ sites with Lewis acidity.

Acetaldehyde, once formed, can be further oxidized into acetic acid. Li and Iglesia [12] reported high selectivity towards acetic acid during the catalytic oxidation of ethanol over Mo-V-Nb mixed-oxide catalysts. The authors also reported a small water inhibition effect on the ethanol oxidation rate, which seems relevant for bioethanol processing, which has a high water content. Other catalysts based on multicomponent mixed oxides have been studied for the conversion of ethanol into acetic acid. In these catalytic systems, oxidation is carried out in the presence of oxygen and takes place in two stages. According to Xiang et al. [13], such a reaction in the presence of air, or even pure oxygen, presents a security issue due to the high flammability of alcohols/oxygen mixtures, but the use of bioethanol can help to overcome such drawback since water will reduce the flammability and explosion issues.

The oxidative dehydrogenation of ethanol to acetaldehyde has been studied since the 1960s and is of great importance today in the biorefinery as a process to valorize bioethanol, which is produced in large quantities from biomass. The typical reaction network for the

dehydrogenative oxidation of ethanol over a wide variety of multicomponent, bulk, and supported metal oxide-based catalysts is that proposed by Pang et al. (Figure 3), where the formation of acetic acid is problematic as it promotes the corrosion of the equipment.

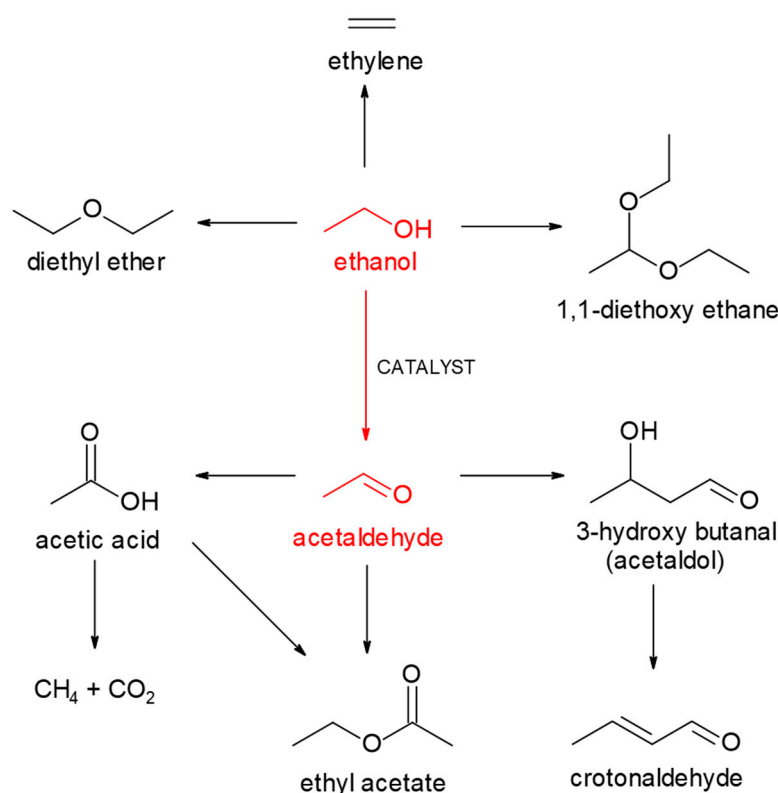


Figure 3. Reaction network for ethanol dehydrogenation into acetaldehyde and byproducts (red) (adapted from [14]).

The catalytic systems described in the literature for the conversion of ethanol into high-value products are numerous, and the identification of the active centers and reaction mechanisms have not been systematized. Given the relevance of bioethanol as a renewable feedstock for the production of highly demanded chemical goods, such as ethylene, the preparation of performant catalysts is relevant to the development of green chemistry processes. In this context, the following sections present data on the catalytic conversion of ethanol over multicomponent catalysts based on Mo, Zr, and W oxides prepared by the combustion of citrate-derived xerogels.

2. Experimental

2.1. Preparation and Characterization of the Catalysts

The catalysts were prepared following a sol-gel-like procedure using citric acid as a complexation agent as described before [15]. The WO₃-ZrO₂ support material (ZrW) was prepared by a sol-gel-like technique in the presence of citric acid (molar ratio Zr/citric acid and W/citric acid = 1). Aqueous solutions of zirconyl chloride and ammonium paratungstate were prepared with an atomic ratio of Zr/W = 1. The solubilization of the zirconyl chloride was achieved by adding HNO₃ (65% w/w solution). The tungsten solution was slowly added to the Zr solution under vigorous stirring. The gel was obtained by evaporating the water by heating it. No precipitation occurs during this step. The gel was dried overnight at 393 K and finally calcined in a muffle at 853 K for 12 h. A yellow-green product was obtained after the calcination step. The deposition of MoO₃, over the calcined support material, was performed by wet impregnation. Aqueous solutions of ammonium heptamolybdate in the presence of citric acid (molar ratio Mo/citric acid = 1) were used. The support material was added to the Mo solution and then the water was evaporated

by heating the suspension under vigorous stirring. After drying overnight (393 K), the samples were calcinated in a muffle (853 K) for 12 h. Since the burning of citrate releases heat, the temperature of powders during calcination will be higher than the ZrO₂ Hüttig temperature (896 K), which is needed for the ZrO₂ agglomerate with WO₃ as reported by Zhou et al. [9]. Samples with 5%, 10%, 20%, and 30% *w/w* of MoO₃/support were prepared. The green shade of the sample intensifies, raising the MoO₃ content. The morphology of fresh catalysts was evaluated by nitrogen adsorption at liquid nitrogen temperature and scanning electron microscopy (SEM). The N₂ physisorption curves were collected using a Perkin–Elmer–Shell 212 C sorptometer (Perkin-Elmer Corporation, Shelton, CT, USA) and data were analyzed using the BET isotherm [16] to compute the surface areas (a_e) of the powders. The SEM micrographs were acquired for samples spread over double-face carbon tape covered by a thin carbon film. A JEOL JSM 840 (JEOL Ltd., Tokyo, Japan) equipment with a Delta KeveX energy-dispersive X-ray analyzer (Kevex Corporation, Foster City, CA, USA) was used to perform chemical analysis (EDS) during image acquisition.

The Raman spectra for fresh catalysts were recorded on a HORIBA LabRam HR Evolution Microscopic Confocal spectrometer (HORIBA, Kyoto, Japan) with a 532 nm argon ion laser.

2.2. Catalytic Tests of Dehydration Dehydrogenation of Ethanol

The ethanol (EtOH) dehydration/dehydrogenation reaction was carried out in a conventional continuous flow apparatus at atmospheric pressure. Catalytic behavior was studied in steady-state conditions. Feed mixtures (6.5%, *v/v*) were prepared by injecting ethanol, or EtOH plus water (water/ethanol = 0.27 *v/v*), into the airflow (35 NL/h) with a precise Gilson 302 pump (Gilson, Wisconsin, WI, USA). The powdered catalysts, $d_p < 125$ nm, (200–900 mg), were diluted with inert SiC (1:4, weight) to avoid adverse thermal effects and charged into a tubular pyrex reactor with a thermocouple in a coaxial-centered thermowell. The reactor outlet was kept at 130 °C to prevent the condensation of liquid products, and was connected to a Shimadzu GC-8A (Shimadzu Corporation, Kyoto, Japan) gas chromatograph with a TCD detector. The carbon balance was evaluated for each catalytic test and the data were rejected if the error was higher than 5%.

3. Results and Discussion

The surface area of fresh catalysts assessed by N₂ physisorption was computed using the BET model. All the characterized materials presented a relatively low surface area because during calcination, the burning of citrate species releases a large amount of heat which promotes sinterization. The data in Figure 4 show that the surface deposition of MoO₃ favors a decrease in the surface area because the MoO₃ crystal promotes the clogging of the pores in the support material. The surface area of the ZrW material is lower than that reported for coprecipitated WO₃-ZrO₂ materials, even when calcined at higher temperatures [17]. For sol-gel WO₃-ZrO₂ mixed oxides, prepared with isopropoxide salts in the presence of isopropanol, Signoretto et al. [18] reported samples having surface areas in the 35–77 m²/g range. The solids calcined at 800 °C showed surface areas that varied with the WO₃ content and on the solvent drying process. More recently, Sarkar et al. [19] referred the production of mesoporous ZrO₂-WO₃ and ZrO₂-MO₃ with large surface areas ($a_e > 200$ m²/g) by a sol-gel procedure using cheap water-soluble salts and a cationic surfactant, which was removed after the gel preparation by a selective extraction procedure. These results underline the sintering effect promoted by citrate burning from the adopted preparation methodology.

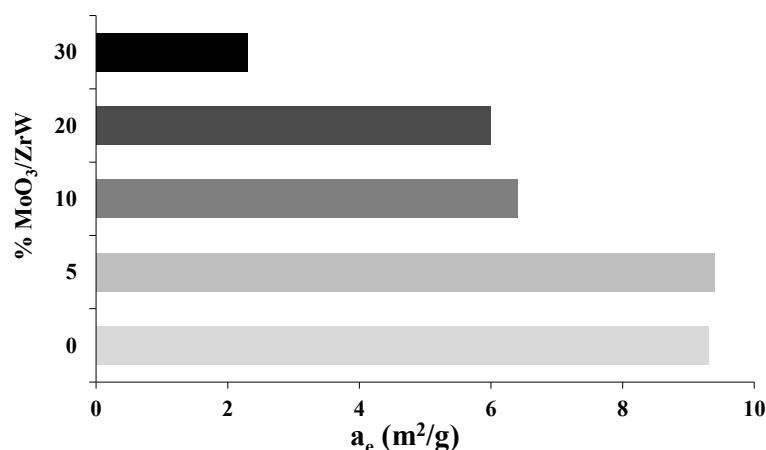


Figure 4. BET surface area of fresh catalysts assessed by N₂ adsorption.

BET data are compatible with the morphology of fresh catalysts analyzed by SEM (Figure 5), which shows the formation of larger agglomerates for samples with larger MoO₃ content. The morphology of the bar ZrW material is slightly different from those reported in the literature due to the unusual preparation methodology adopted and high WO₃ content. The crystallite clusters in Figure 5 are two orders of magnitude larger than those reported by Chen et al. [20], which is because materials that have a high WO₃ content have a relatively low Tammann temperature, and, therefore, promotes sintering during the annealing treatment. EDS elemental analysis in Table 2 shows that elongated agglomerates in the ZrW material are W-rich and seem to vanish for the post-reaction sample, maybe due to recrystallization or/and sublimation. For samples containing MoO₃, data in Table 2 show that MoO₃ is located over the surface because Mo content is always higher than the value used in the sample preparation, which was computed as a bulk content. This result is visible in the 5% MoO₃ sample, which has almost twice as much Mo in the EDS elemental analysis (average value of 9.1% instead of 5%).

Table 2. EDS elemental analysis of fresh catalysts with low and high MoO₃ contents (analysis performed in different points).

Atomic (%)	Catalysts						
	0% MoO ₃			5% MoO ₃			30% MoO ₃
Point	#1	#2	#3	#1	#2	#3	#1
Zr	46.3	42.6	28.2 *	25.0	12.0	12.2	28.4
W	53.7	57.4	71.8 *	67.5	78.8	77.3	27.3
Mo	0.0	0.0	0.0	7.5	9.2	10.5	44.3

* Needle-shaped agglomerate.

The XRD patterns of fresh catalysts, Figure 6, show XRD diffraction lines mainly ascribable to monoclinic WO₃ [21] overlaid with XRD lines of mixed Mo-W oxide, which is formed due to the resemblance between W⁶⁺ and Mo⁶⁺ in valence, electronegativity, and ionic radius (W⁶⁺, 74 pm; Mo⁶⁺, 73 pm) [22]. The bar ZrW sample presents a low intensity and broad diffraction line around 30° [23], which seems to indicate the presence of nanostructured tetragonal zirconia. The diffraction lines for zirconia are not particularly noticeable, which is attributable in part to the fact that this phase has a lower mass than the total of the W and Mo oxides.

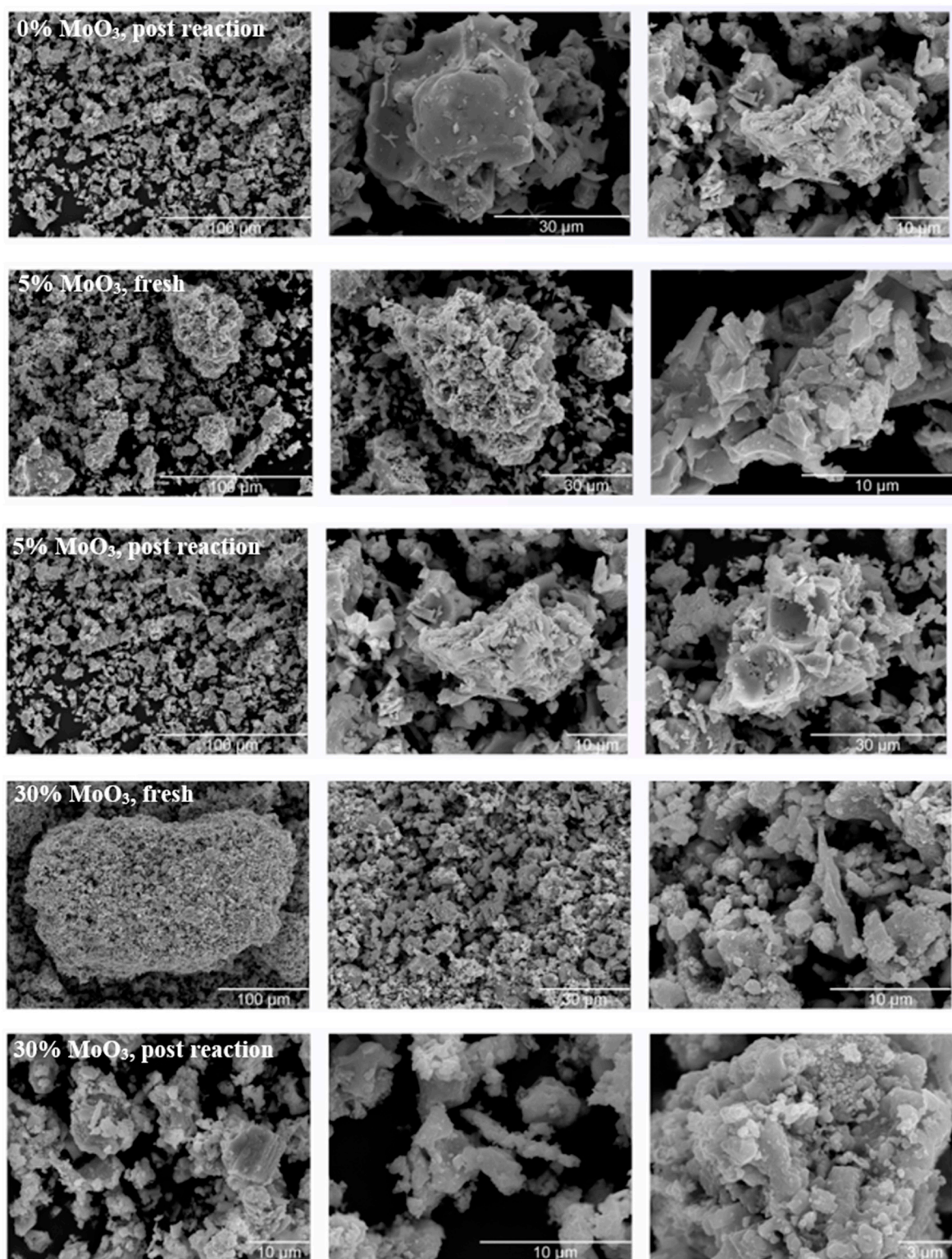


Figure 5. SEM micrographs of fresh and post-reaction catalysts with low and high MoO₃ contents.

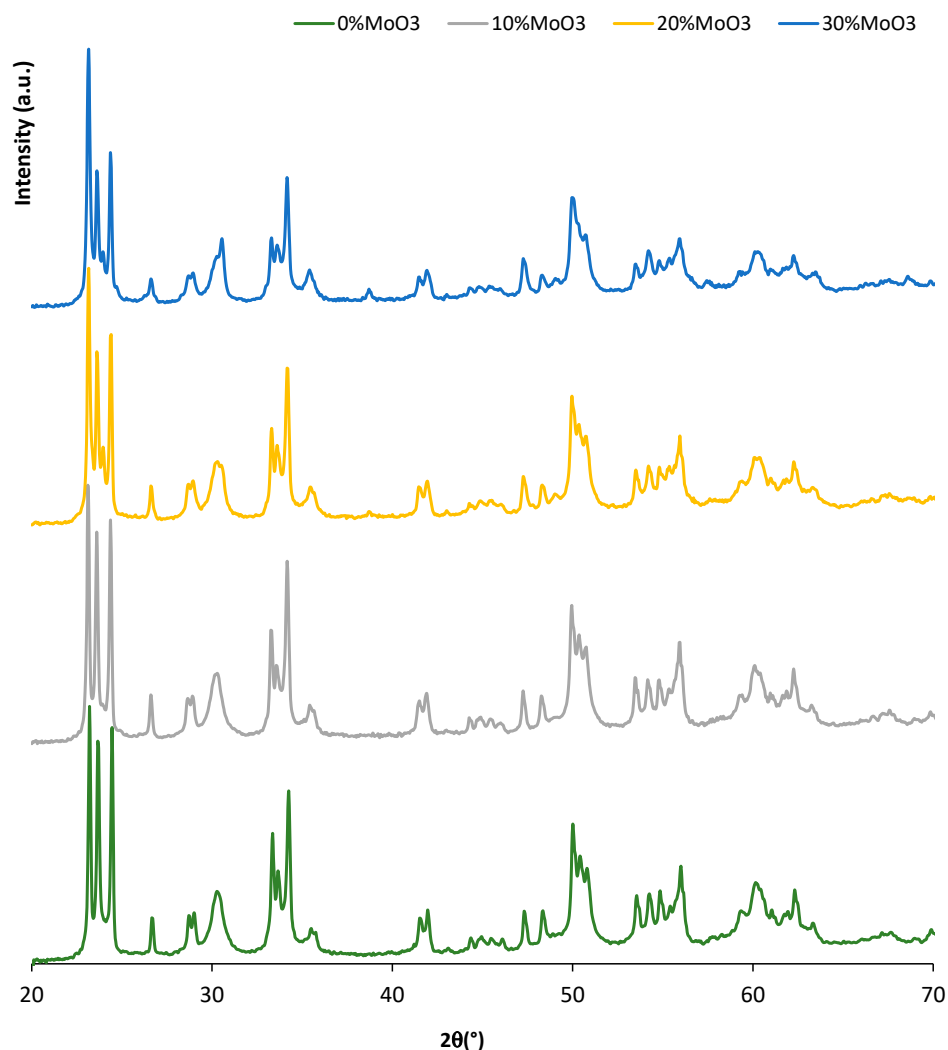


Figure 6. XRD patterns of fresh catalysts.

The Raman spectra of fresh catalysts (Figure 7) are dominated by the Raman features of crystalline WO_3 (803 , 711 , 324 , and 270 cm^{-1}), which is typical of $\text{WO}_3\text{-ZrO}_2$ materials with WO_3 loads beyond a certain value (above the WO_3 monolayer level) [24]. The sample with high MoO_3 loadings show shoulders around 838 cm^{-1} and 742 cm^{-1} attributable to mixed oxides $\text{Mo}_{1-x}\text{W}_x\text{O}_3$, as reported by Kondrachova et al. [25].

The catalytic behavior of the prepared catalysts was evaluated for ethanol conversion in oxidative conditions. The gas phase process was carried out using air as an oxidant and the main data on the catalytic behavior are displayed in Figure 8. As expected, due to its high acidity, the ZrW catalyst, with 0% of MoO_3 , mainly produces ethylene by dehydration [8]. The selectivity towards ethylene is favoured by reaction temperature due to the endothermic character of the dehydration reaction ($\text{DH}_{298\text{ K}} = 45\text{ kJ/mol}$) [8]. For the lowest tested temperature ($280\text{ }^\circ\text{C}$), appreciable production of acetic acid was obtained (selectivity of 35.3%), which arises from consecutive oxidation of the formed acetaldehyde which has the same reaction intermediate than ethylene [11]. Increasing reaction temperature, the conversion and the selectivity toward ethylene increase, and the selectivity toward acetic acid decreases. The ZrW-tested catalyst presented catalytic performances like those of protonic catalysts with Brönsted acidity [8]. For ZrW catalysts, the Brönsted acid sites are related to hydroxylated phases, which can be formed during the reaction since water is formed for each ethanol molecule converted [14]. The catalysts with high MoO_3 contents presented acetaldehyde as the main reaction product due to the high reducibility of Mo^{6+} species on the catalyst surface [10]. For the same surface

area, the catalysts containing MoO₃ are less active than the bar ZrW one (Figure 9). The catalytic activity decreases as the molybdenum content increases because surface acidity decreases as the Mo content increases. This is accompanied by an increase in selectivity for total oxidation products (CO_x = CO + CO₂) and a slight increase in selectivity for acetaldehyde. The observed result is consistent with the findings of Rousseau et al. [10], who found that stronger Lewis acidity of the W⁶⁺ sites relative to the Mo⁶⁺ increases overall reactivity. Still, the more readily reducible Mo⁶⁺ leads to a higher selectivity towards oxidation reactions. The oxidative dehydrogenation of ethanol into acetaldehyde is an exothermic process (DH_{298 K} = 179 kJ/mol) [26]; hence, the rise of the reaction temperature is unfavourable. The acetaldehyde selectivity achieved by the multicomponent mixed-oxide catalysts studied was comparable to those produced by noble metal catalysts. The use of non-noble metals is attractive for economic and environmental reasons [27].

Catalysts containing MoO₃ show a loss of Mo in the reaction conditions. The reactor (pyrex) bottom was blue after the reaction, indicating the formation of Mo volatile species during the reaction. The effect was more pronounced for the catalysts with a high Mo content. The post-reaction catalysts show a color change, which seems to indicate that Mo⁶⁺ was partially reduced to Mo⁵⁺, which according to Chan et al. [14], is not a catalyst deactivation source because the Mo⁶⁺/Mo⁵⁺ species are still as active in alcohol dehydrogenation as the Mo⁶⁺ species. However, data in Figure 10 show a drop in acetaldehyde selectivity, raising the ethanol conversion because the Mo⁶⁺/Mo⁵⁺ species form tetrahedral MoO_x with Brönsted acidity [28], which improves the dehydration ability responsible for the increase in ethylene selectivity. Also, the formed acetaldehyde can be converted into CO_x through consecutive oxidation reactions [14]. For the bar ZrW catalyst, the selectivity towards ethylene also increases, raising the ethanol conversion, because the slight reduction in W⁶⁺ species during the reaction promotes the formation of WO_x clusters with improved Brönsted acidity [29]. The partial reduction in W⁶⁺ was responsible for the grey color, instead of yellow, of the post-reaction sample. Also, the formation of hydroxylated phases during the reaction contributes to the selectivity increase [14].

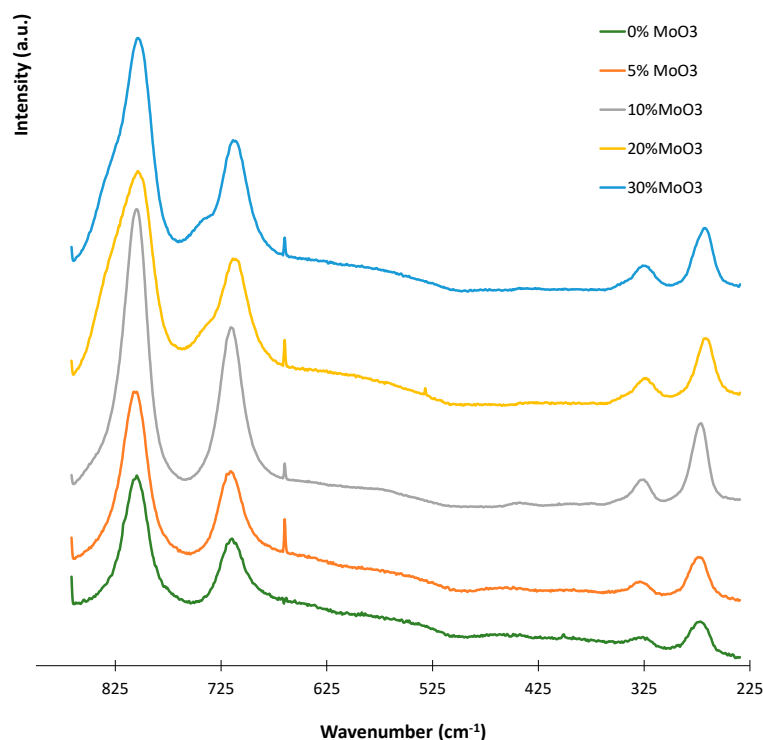


Figure 7. Raman spectra of fresh catalysts.

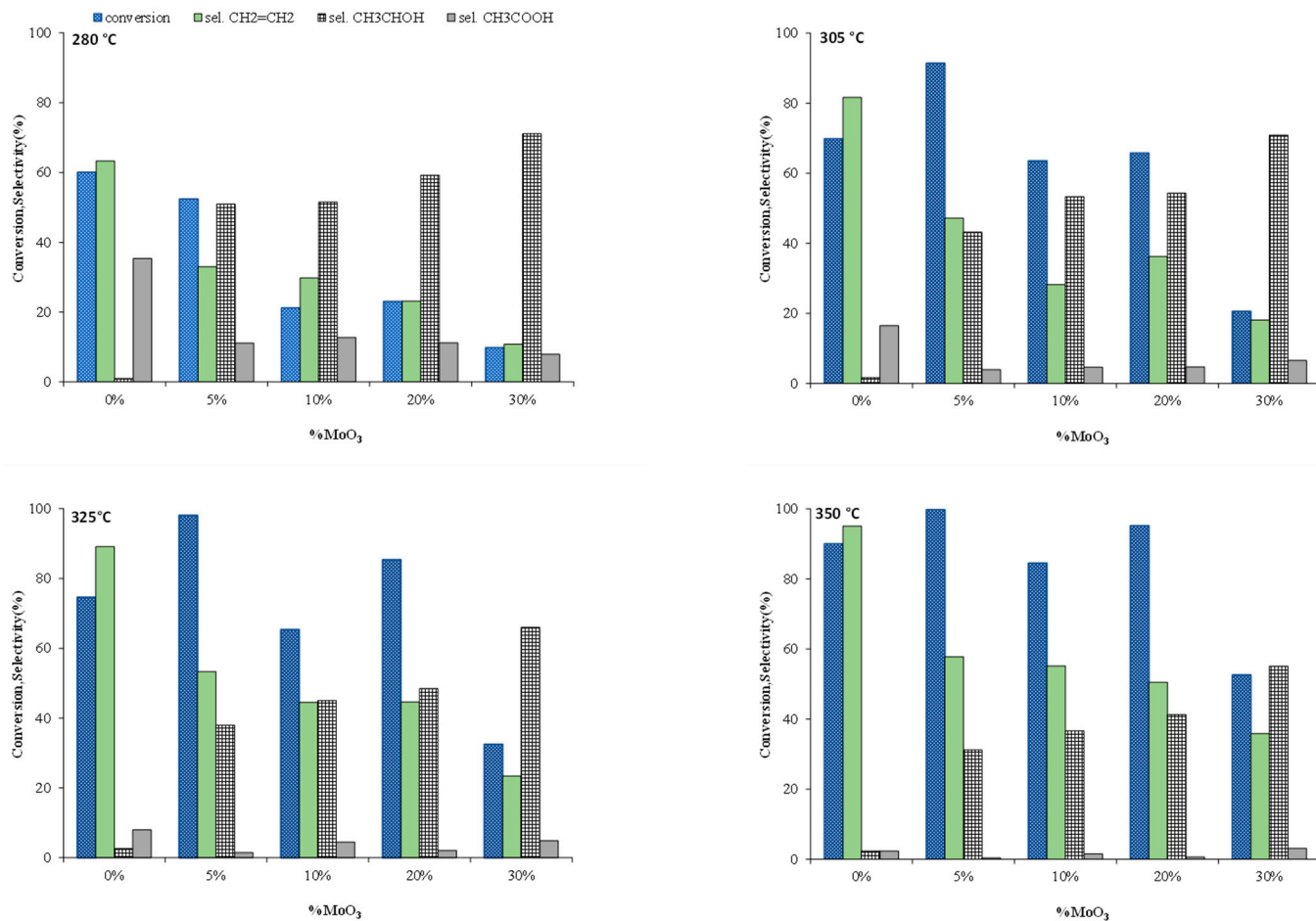


Figure 8. Temperature effect on the catalytic performances of prepared catalysts (catalysts 900 mg).

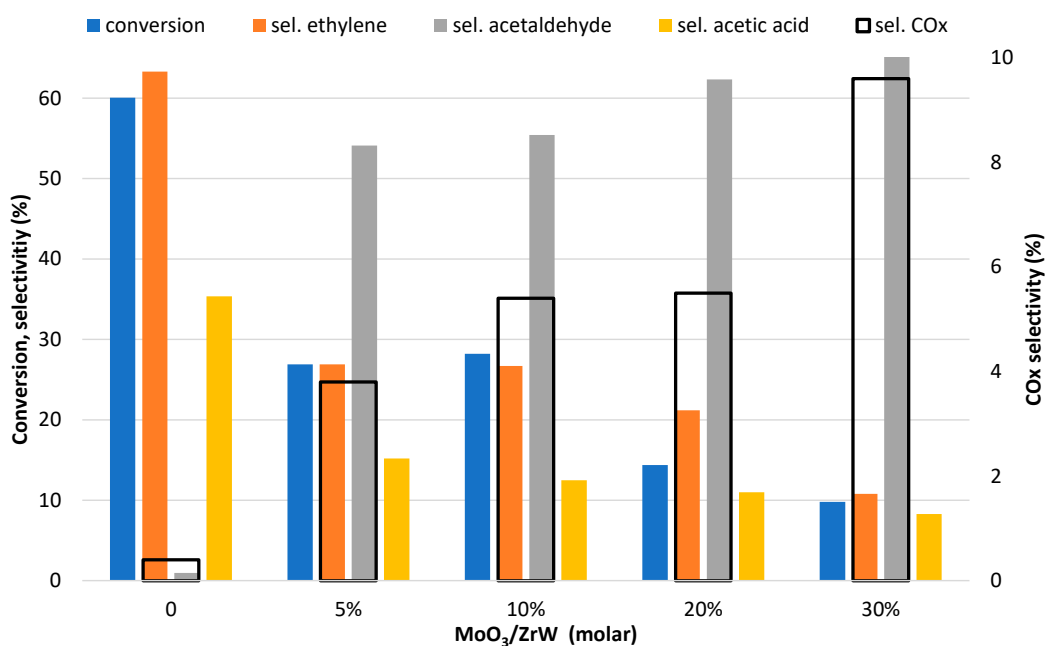


Figure 9. Catalytic performances of catalysts for the same surface area (2 m²), at 280 °C and 6.5% of ethanol in air (v/v).

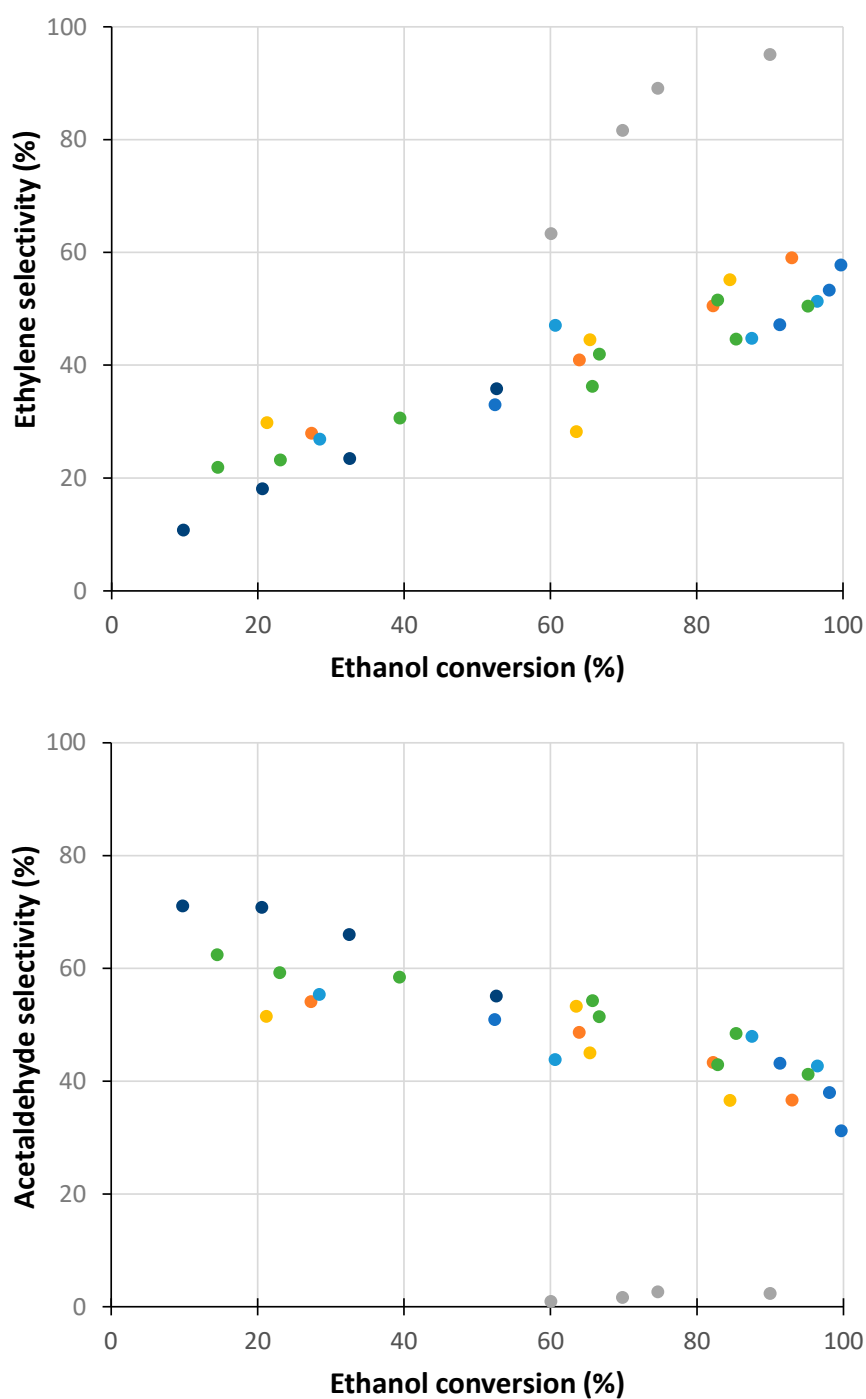


Figure 10. Acetaldehyde and ethylene selectivities versus ethanol conversion (●—0% MoO₃; colored dots for catalysts with MoO₃).

Given that bioethanol can contain high concentrations of water, the catalytic behavior during the processing of ethanol with a high water content (27% molar) was studied for the 5% MoO₃ catalyst sample. The data in Figure 11 show that the introduction of water, simulating bioethanol, has only a slightly inhibitory effect, which is because alcohol and water can adsorb competitively on the active centers of the catalyst, as reported for methanol/water for the Mo-Fe-O catalyst [30]. Moreover, the dehydration and oxidative dehydrogenation of ethanol produces water, which is why the water concentration in the reaction medium is always high, even when dried ethanol is used.

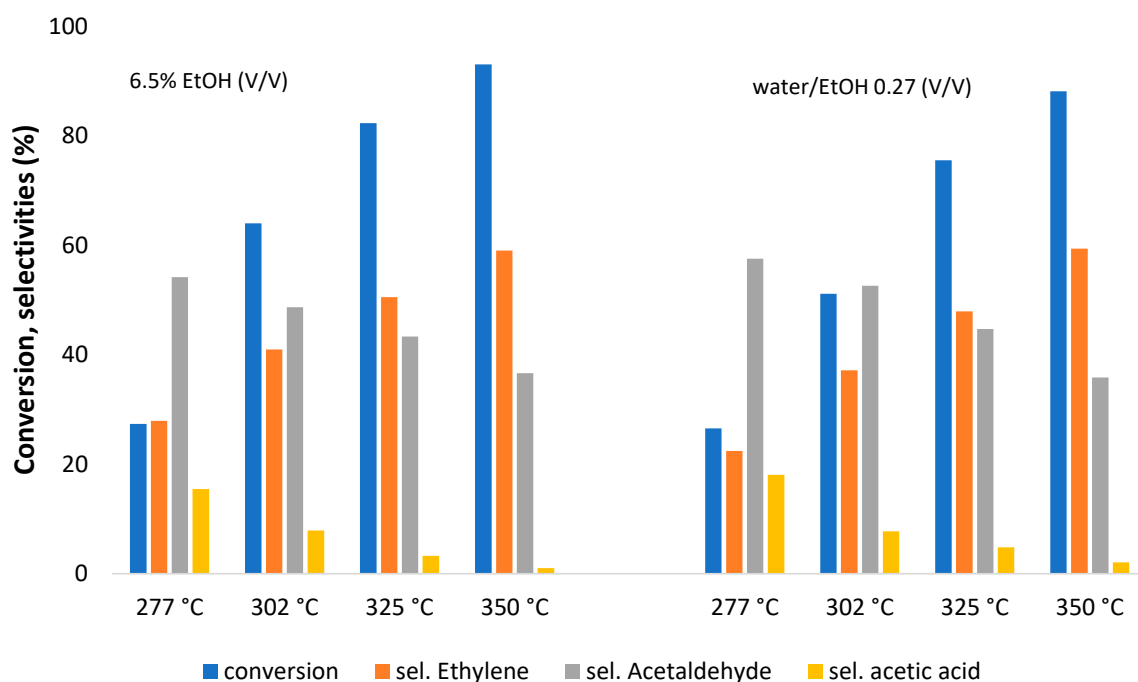


Figure 11. Water effect (simulation of bioethanol) on the catalytic performances of the 5% MoO₃ catalyst (w = 226.5 mg).

4. Conclusions

The preparation of ZrW mixed oxides by the citrate route led to low surface area materials with tetragonal nanostructured zirconia and large WO₃ crystals resulting from the conjunction of the heat released in the burning of the citrates and the relatively low Tammann temperature of the WO₃. The material showed high catalytic activity for ethanol dehydration into ethylene accompanied, at the low reaction temperature, by the significant production of acetic acid which causes corrosion issues. The surface deposition of MoO₃ on the ZrW material leads to a decrease in acidity and an improvement in redox properties, leading to high selectivities for acetaldehyde produced by ethanol oxidative dehydrogenation. Acetic acid production is minimal on Mo-modified catalysts. The results show that multicomponent Mo-W-Zr-based oxide catalysts are versatile for the valorization of bioethanol as they are not very sensitive to water, and their selectivity for dehydration/dehydrogenation can be tuned depending on the Mo content. With various economic and environmental advantages, these catalysts compete with those based on noble metals for the dehydration of ethanol to acetaldehyde.

Author Contributions: Conceptualization, A.P.S.D. and B.R.; methodology, A.P.S.D., B.R. and M.F.C.P.; formal analysis, O.D.P., R.Z. and M.F.C.P.; investigation, A.P.S.D., B.R. and M.F.C.P.; resources, A.P.S.D.; data curation, R.Z. and O.D.P.; writing—original draft preparation, A.P.S.D., B.R.; writing—review and editing, A.P.S.D., B.R. and R.Z. All authors have read and agreed to the published version of the manuscript.

Funding: This work was partially supported through the FCT strategic funding of CERENA (UIDB/04028/2020).

Data Availability Statement: Data will be made available on request.

Conflicts of Interest: The authors declare no conflict of interest.

References

1. Rosales-Calderon, O.; Arantes, V. A review on commercial-scale high-value products that can be produced alongside cellulosic ethanol. *Biotechnol. Biofuels* **2019**, *12*, 240. [CrossRef]
2. Posada, J.A.; Patel, A.D.; Roes, A.; Blok, K.; Faaij, A.P.; Patel, M.K. Potential of bioethanol as a chemical building block for biorefineries: Preliminary sustainability assessment of 12 bioethanol-based products. *Bioresour. Technol.* **2013**, *135*, 490–499. [CrossRef]
3. Dagle, R.A.; Winkelman, A.D.; Ramasamy, K.K.; Dagle, V.L.; Weber, R.S. Ethanol as a Renewable Building Block for Fuels and Chemicals. *Ind. Eng. Chem. Res.* **2020**, *59*, 4843–4853. [CrossRef]
4. Frosi, M.; Tripodi, A.; Conte, F.; Ramis, G.; Mahinpey, N.; Rossetti, I. Ethylene from renewable ethanol: Process optimization and economic feasibility assessment. *J. Ind. Eng. Chem.* **2021**, *104*, 272–285. [CrossRef]
5. He, L.; Zhou, B.-C.; Sun, D.-H.; Li, W.-C.; Lv, W.-L.; Wang, J.; Liang, Y.-Q.; Lu, A.-H. Catalytic Conversion of Ethanol to Oxygen-Containing Value-Added Chemicals. *ACS Catal.* **2023**, *13*, 11291–11304. [CrossRef]
6. Shinohara, Y.; Nakajima, T.; Suzukia, S.; Mishimab, S.; Ishikawac, H. A Computational Chemical Investigation of the Dehydration and Dehydrogenation of Ethanol on Oxide Catalysts. *J. Chem. Softw.* **1998**, *4*, 89–100. Available online: https://web.archive.org/web/20181102054541id_/https://www.jstage.jst.go.jp/article/jchemsoft1992/4/3/4_3_89/_pdf (accessed on 10 December 2023). [CrossRef]
7. Mabate, T.P.; Maqunga, N.P.; Ntshibongo, S.; Maumela, M.; Bingwa, N. Metal oxides and their roles in heterogeneous catalysis: Special emphasis on synthesis protocols, intrinsic properties, and their influence in transfer hydrogenation reactions. *SN Appl. Sci.* **2023**, *5*, 196. [CrossRef]
8. Phung, T.K.; Hernández, L.P.; Busca, G. Conversion of ethanol over transition metal oxide catalysts: Effect of tungsta addition on catalytic behaviour of titania and zirconia. *Appl. Catal. A Gen.* **2015**, *489*, 180–187. [CrossRef]
9. Zhou, W.; Soutanidis, N.; Xu, H.; Wong, M.S.; Neurock, M.; Kiely, C.J.; Wachs, I.E. Nature of Catalytically Active Sites in the Supported WO_3/ZrO_2 Solid Acid System: A Current Perspective. *ACS Catal.* **2017**, *7*, 2181–2198. [CrossRef]
10. Rousseau, R.; Dixon, D.A.; Kay, B.D.; Dohnálek, Z. Dehydration, dehydrogenation, and condensation of alcohols on supported oxide catalysts based on cyclic $(\text{WO}_3)_3$ and $(\text{MoO}_3)_3$ clusters. *Chem. Soc. Rev.* **2014**, *43*, 7664–7680. [CrossRef] [PubMed]
11. Chuklina, S.; Chuklina, S.; Zhukova, A.; Zhukova, A.; Fionov, Y.; Fionov, Y.; Kadyko, M.; Kadyko, M.; Fionov, A.; Fionov, A.; et al. Selectivity of Ethanol Conversion on Al/Zr/Ce Mixed Oxides: Dehydration and Dehydrogenation Pathways Based on Surface Acidity Properties. *ChemistrySelect* **2022**, *7*, e202203031. [CrossRef]
12. Li, X.; Iglesia, E. Selective Catalytic Oxidation of Ethanol to Acetic Acid on Dispersed Mo-V-Nb Mixed Oxides. *Chem.–A Eur. J.* **2007**, *13*, 9324–9330. [CrossRef]
13. Xiang, N.; Xu, P.; Ran, N.; Ye, T. Production of acetic acid from ethanol over CuCr catalysts via dehydrogenation-(aldehyde–water shift) reaction. *RSC Adv.* **2017**, *7*, 38586–38593. [CrossRef]
14. Pang, J.; Yin, M.; Wu, P.; Li, X.; Li, H.; Zheng, M.; Zhang, T. Advances in catalytic dehydrogenation of ethanol to acetaldehyde. *Green Chem.* **2021**, *23*, 7902–7916. [CrossRef]
15. Dias, A.P.S.; Dimitrov, L.D.; Oliveira, M.C.-R.; Zăvoianu, R.; Fernandes, A.; Portela, M.F. Oxidative dehydrogenation of butane over substoichiometric magnesium vanadate catalysts prepared by citrate route. *J. Non-Crystalline Solids* **2010**, *356*, 1488–1497. [CrossRef]
16. Thommes, M.; Kaneko, K.; Neimark, A.V.; Olivier, J.P.; Rodriguez-Reinoso, F.; Rouquerol, J.; Sing, K.S.W. Physisorption of gases, with special reference to the evaluation of surface area and pore size distribution (IUPAC Technical Report). *Pure Appl. Chem.* **2015**, *87*, 1051–1069. [CrossRef]
17. Kourieh, R.; Bennici, S.; Marzo, M.; Gervasini, A.; Auroux, A. Investigation of the WO_3/ZrO_2 surface acidic properties for the aqueous hydrolysis of cellobiose. *Catal. Commun.* **2012**, *19*, 119–126. [CrossRef]
18. Signoreto, M.; Scarpa, M.; Pinna, F.; Strukul, G.; Canton, P.; Benedetti, A. WO_3/ZrO_2 catalysts by sol–gel processing. *J. Non-Cryst. Solids* **1998**, *225*, 178–183. [CrossRef]
19. Sarkar, A.; Pramanik, S.; Achariya, A.; Pramanik, P. A novel sol–gel synthesis of mesoporous $\text{ZrO}_2\text{–MoO}_3/\text{WO}_3$ mixed oxides. *Microporous Mesoporous Mater.* **2008**, *115*, 426–431. [CrossRef]
20. Chen, S.; Wang, W.; Zhang, Y.; Wei, Y.; Fang, W.; Yang, Y. Thiolation of dimethyl sulfide to methanethiol over WO_3/ZrO_2 catalysts. *J. Mol. Catal. A Chem.* **2012**, *365*, 60–65. [CrossRef]
21. Zhang, H.; Liu, B.; Lv, L.; Shao, J.; Du, Y.; Li, Y.; Chang, W. Enhanced triethylamine sensing characteristics of In-doped WO_3 cubic nanoblocks at low operating temperature. *Vacuum* **2023**, *218*, 112640. [CrossRef]
22. Zhou, H.; Zou, X.; Zhang, K.; Sun, P.; Islam, S.; Gong, J.; Zhang, Y.; Yang, J. Molybdenum–Tungsten Mixed Oxide Deposited into Titanium Dioxide Nanotube Arrays for Ultrahigh Rate Supercapacitors. *ACS Appl. Mater. Interfaces* **2017**, *9*, 18699–18709. [CrossRef] [PubMed]
23. Liu, C.; Sun, J.; Brown, H.M.; Marin-Flores, O.G.; Bays, J.T.; Karim, A.M.; Wang, Y. Aqueous phase hydrodeoxygenation of polyols over Pd/ $\text{WO}_3\text{–ZrO}_2$: Role of Pd- WO_3 interaction and hydrodeoxygenation pathway. *Catal. Today* **2016**, *269*, 103–109. [CrossRef]
24. Zhao, B.; Xu, X.; Gao, J.; Fu, Q.; Tang, Y. Structure Characterization of WO_3/ZrO_2 Catalysts by Raman Spectroscopy. *J. Raman Spectrosc.* **1996**, *27*, 549–554. [CrossRef]
25. Kondrachova, L.; Hahn, B.P.; Vijayaraghavan, G.; Williams, R.D.; Stevenson, K.J. Cathodic Electrodeposition of Mixed Molybdenum Tungsten Oxides from Peroxo-polymolybdotungstate Solutions. *Langmuir* **2006**, *22*, 10490–10498. [CrossRef] [PubMed]

26. Lee, J.-H.; Shin, C.-H.; Suh, Y.-W. Higher Brønsted acidity of WO_x/ZrO_2 catalysts prepared using a high-surface-area zirconium oxyhydroxide. *Mol. Catal.* **2017**, *438*, 272–279. [[CrossRef](#)]
27. Chan, X.; Akter, N.; Yang, P.; Ooi, C.; James, A.; Boscoboinik, J.A.; Parise, J.B.; Kim, T. Fundamental study of furfuryl alcohol dehydration reaction over molybdenum oxide catalyst. *Mol. Catal.* **2019**, *466*, 19–25. [[CrossRef](#)]
28. Hahn, T.; Bentrup, U.; Armbrüster, M.; Kondratenko, E.V.; Linke, D. The Enhancing Effect of Brønsted Acidity of Supported MoO_x Species on their Activity and Selectivity in Ethylene/*trans*-2-Butene Metathesis. *ChemCatChem* **2014**, *6*, 1664–1672. [[CrossRef](#)]
29. Barton, D.G.; Soled, S.L.; Iglesia, E. Solid acid catalysts based on supported tungsten oxides. *Top. Catal.* **1998**, *6*, 87–99. [[CrossRef](#)]
30. Dias, A.P.S.; Rijo, B.; Kiennemann, A.; Portela, M.F. Methanol oxidation over iron molybdate catalysts. Main and side reactions kinetics. *Appl. Catal. A Gen.* **2023**, *658*, 119118. [[CrossRef](#)]

Disclaimer/Publisher’s Note: The statements, opinions and data contained in all publications are solely those of the individual author(s) and contributor(s) and not of MDPI and/or the editor(s). MDPI and/or the editor(s) disclaim responsibility for any injury to people or property resulting from any ideas, methods, instructions or products referred to in the content.